

EFFECTS OF REVERSE RADIATION NOISE ON MILLIMETER-WAVE RADIOMETRIC IMAGING AT SHORT RANGE

T.-Y. Hu^{*}, Z.-L. Xiao, J.-Z. Xu, and L. Wu

School of Electronic Engineering and Optoelectronic Technology, Nanjing University of Science and Technology, Nanjing 210094, China

Abstract—The existence of reverse radiation noise in the millimeter-wave (MMW) radiometric imaging system with a superheterodyne receiver seriously affects the imaging experiments carried out at short range, thus leading to the degradation of MMW radiometric images and difficulty in recognizing targets. Based on the generation mechanism of reverse radiation noise, the specific influence on imaging for relative radiometry is investigated in this paper, and some methods of eliminating or reducing this noise are proposed. Then, two series of comparative imaging experiments are conducted with a 3 mm band radiometric imaging system. Both theoretical analysis and experimental results are presented to validate the actual existence of interference-like stripes imposed by the reverse radiation noise. Moreover, it is proved that adopting an isolator in the MMW receiving front-end can effectively reduce the reverse radiation noise and significantly improve the imaging performance.

1. INTRODUCTION

Millimeter-wave (MMW) radiometric imaging is a thermal imaging technique, and it generates interpretable images through collecting the naturally occurring MMW radiation energy from the scene under observation [1]. When compared with active imaging, MMW radiometric imaging does not radiate any form of radiation, and it offers the advantages of imaging covertly, eliminating specular effects and avoidance of interference with other systems [2]. Additionally, due to the superior capability of imaging through natural and manmade

Received 26 September 2011, Accepted 17 October 2011, Scheduled 25 October 2011

* Corresponding author: Taiyang Hu (sun1983hu@126.com).

obscurants, MMW radiometric imaging has attracted increasing attention in broad areas ranging from precise guidance to concealed contraband detection [3–7].

The critical part in a MMW radiometric imaging system is the MMW radiometer, which is essentially a highly sensitive receiver [8] and usually adopts the superheterodyne mode. During the practical imaging experiments carried out at a short range (about 1–2 m), it is found that the output signal of imaging system sometimes does not follow with the changes of the object's radiation characteristics, and there exists phenomenon just like the specular reflection in a radar detection system, both of which arise from the internally generated reverse radiation noise. Reverse radiation noise is referred to the noise power radiated by a receiver via antenna, which is reflected by objects of being imaged and in turn collected by the receiving antenna again. Along with the normal thermal MMW radiation energy, the flow of reflected noise power enters into the receiving channel and will seriously affect the imaging performance when it reaches a certain degree. Therefore, it is essential to study the generation and transfer mechanism of reverse radiation noise, as well as the methods of eliminating or reducing this noise. Peng et al. [9] have analyzed the effect of reverse radiation noise on antenna temperature calibration in a microwave radiometer for remote sensing. Li et al. [10] have studied the influence of reverse radiation on the calibration of microwave radiometer and the ground-based microwave radiation measurement near nadir angle. Li et al. [11] have examined the effect of reverse radiometer thermal noise in microwave radiometer on antenna calibration through simulation in CST. However, these works are primarily related with theoretical analysis and computer simulation, and the applied backgrounds of them belong to the category of absolute radiometry, such as remote sensing, oceanographic observation, and radio astronomy observation, all of which measure the absolute radiometric temperatures. Besides, as to the influences of reverse radiation noise on MMW radiometric imaging for relative radiometry, which refers to imaging through exploiting the relative difference in radiometric temperatures between the objects and backgrounds under observation, such as concealed contraband detection, they have rarely been reported in literatures, and the corresponding theoretical and experimental researches should be put into practice.

In this paper, the specific influence of reverse radiation noise on MMW radiometric imaging for relative radiometry at short range is investigated. Then, some methods of eliminating or reducing this noise are analyzed and compared. Moreover, in order to confirm the actual existence of interference-like stripes imposed by reverse radiation noise,

two series of comparative imaging experiments are performed indoors. In the meantime, the feasibility and significance of adopting an isolator in the MMW front-end for reducing this noise are also verified.

2. GENERATION MECHANISM OF REVERSE RADIATION NOISE

The radiometric temperature contrast is of great interest from the viewpoint of enhancing the detection and recognition probability in concealed contraband detection [12], which pertains to the category of relative radiometry. The total-power MMW radiometer with a superheterodyne receiver is usually applied in the area of concealed contraband detection, and its principle block diagram is shown in Figure 1.

As shown in Figure 1, the incident MMW radiation energy from objects and backgrounds within the imaging scene is collected by an antenna, and then the radiation energy is transformed into a direct-current (DC) voltage after the processing of mixing, amplification, filtering, and square-law detection [8]. Meanwhile, the output voltage that is linearly proportional to the collected radiation energy is sampled and transformed into gray-scale or pseudo-color images. The reverse radiation noise is composed of three parts: the modulation noise and narrowband leakage of local oscillator (LO) leaking from LO port to RF port of the mixer, the noise of pre-intermediate frequency (IF) amplifier leaking from IF port to RF port, and the noise of mixer leaking to RF port. Among the three parts presented above, the first part plays an important role for generating reverse radiation noise. Then, the noise of pre-IF amplifier is equivalent to the thermal noise introduced by the reverse attenuation between IF port and RF port. Finally, the noise arising from the mixer itself is insignificant when compared with the former two parts, and can be neglected.

According to [9], the mixer can be considered as an attenuator to the radiation noise transmitting reversely, and the attenuation value of the LO-RF port in a double-sideband receiving system is half of

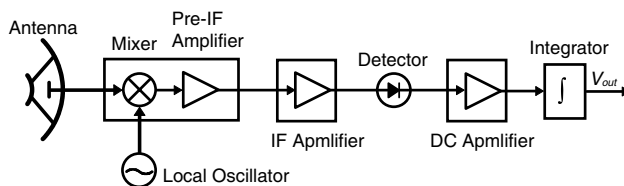


Figure 1. Block diagram of total-power superheterodyne radiometer.

the LO-RF port isolation, as it is for the IF-RF port. Meanwhile, the noise power can be characterized by an equivalent noise temperature in radiometry [8]. Hence, as for a double-sideband radiometer, the reverse radiation noise arriving at the RF port of mixer is described by the following expression:

$$T_{RN} = \frac{2T_{ON}}{L_{OR}} + \left(1 - \frac{2}{L_{OR}}\right)T_0 + \left(1 - \frac{2}{L_{IR}}\right)T_0 \quad (1)$$

where T_{ON} is the equivalent modulation and leakage noise temperature of LO, T_0 is the physical temperature, L_{OR} is the LO-RF port isolation, and L_{IR} is the IF-RF port isolation. For convenience, let $L_{OR} = L_{IR}$, and Equation (1) can be rewritten as:

$$T_{RN} = \frac{2T_{ON}}{L_{OR}} + 2\left(1 - \frac{2}{L_{OR}}\right)T_0 \quad (2)$$

The equivalent modulated and leaked noise temperature of LO T_{ON} is defined as:

$$T_{ON} = \frac{P_{LO}}{k}\zeta_{IF} \quad (3)$$

where P_{LO} is the power of LO, k is Boltzmann's constant, and ζ_{IF} is the equivalent integrated factor of LO for generating reverse radiation noise over the range of IF bandwidth.

When imaging experiments are conducted at short range, the footprint projected by a MMW antenna is usually smaller than the object area due to the narrow antenna beamwidth at MMW band, and the noise temperature reflected back by the objects and received by the antenna again is represented by:

$$T_{RR} = \frac{T_{RN}G^2\lambda^2\sigma\rho}{64\pi^3R^4} \quad (4)$$

where G is the antenna gain, λ is the center wavelength of receiver, σ is the footprint area of antenna, R is the detection distance, and ρ is the reflectivity of object or background.

When $\rho = 1$, Equation (4) reduces to:

$$T_{RA} = T_{RR}|_{\rho=1} = \frac{T_{RN}G^2\lambda^2\sigma}{64\pi^3R^4} = T_{RN}\psi \quad (5)$$

where $\psi = (G^2\lambda^2\sigma)/(64\pi^3R^4)$ is designated as the receiving factor.

If the half-power beamwidth of antenna is denoted by $\theta_{3\text{dB}}$, then the footprint area of antenna can be given by:

$$\sigma = \pi \left(\frac{\theta_{3\text{dB}}\pi R}{360}\right)^2 \quad (6)$$

Therefore, substituting Equations (2), (3) and (6) into Equation (5) gives:

$$T_{RA} = \frac{G^2 \lambda^2 [P_{LO} \zeta_{IF} + k(L_{OR} - 2)T_0]}{32R^2 k L_{OR}} \cdot \left(\frac{\theta_{3\text{dB}}}{360} \right)^2 \quad (7)$$

3. EFFECTS AND REDUCTION OF REVERSE RADIATION NOISE

MMW radiometric imaging generates images depending on the distinctive radiation characteristics of the different objects and backgrounds under observation. When the imaging system detects objects within a short range, the antenna temperature contrast between the object and the background is expressed as:

$$\Delta T_A = T_{APt} - T_{APb} \quad (8)$$

where T_{APt} and T_{APb} denote the apparent temperature distribution of object and background, respectively.

According to [12], T_{APt} and T_{APb} can be described as follows:

$$T_{APt} = \rho_t(T_{RA} + T_S) + e_t T_t \quad (9)$$

$$T_{APb} = \rho_b(T_{RA} + T_S) + e_b T_b \quad (10)$$

Taking the reverse radiation noise into account, the antenna temperature contrast can be rewritten through substituting Equations (9) and (10) into Equation (8), and the result is:

$$\Delta T_A = (\rho_t - \rho_b)T_{RA} + (\rho_t - \rho_b)T_S + e_t T_t - e_b T_b \quad (11)$$

where ρ_t , e_t , and T_t are, respectively, the reflectivity, emissivity and physical temperature of object. And at the same time, ρ_b , e_b , and T_b are the reflectivity, emissivity and physical temperature of object, respectively. In addition, T_S denotes the radiometric temperature of surroundings.

From the discussion presented above, it is noted that Equation (11) constitutes the theoretical basis of MMW radiometric imaging for relative radiometry. Additionally, the first part in Equation (11) reveals the specific influence on antenna temperature contrast resulted from the reverse radiation noise, and it is list as below:

$$\Delta T_{AR} = (\rho_t - \rho_b) \cdot \frac{G^2 \lambda^2 [P_{LO} \zeta_{IF} + k(L_{OR} - 2)T_0]}{32R^2 k L_{OR}} \cdot \left(\frac{\theta_{3\text{dB}}}{360} \right)^2 \quad (12)$$

Considering Equation (12), ρ_t is generally not equal to ρ_b , and ρ_t approaches 1 when the object under observation is bare metal. So the influence of reverse radiation noise on antenna temperature

contrast cannot be neglected, and it is mainly related to the half-power beamwidth of antenna $\theta_{3\text{dB}}$, the equivalent integrated factor of LO ζ_{IF} , and the LO-RF port isolation L_{OR} , when the detection distance R is fixed.

Referring to the theory of relative radiometry coupled with Equation (11), it is evident that the differences in antenna temperature are beneficial to the discrimination of objects among one another and from the background. Hence, the reverse radiation noise is helpful for MMW radiometric imaging in the perspective of theoretical analysis, and this phenomenon is similar to the method of enhancing imaging performance through increasing the radiometric temperature contrast via artificial illumination [12].

However, due to the mismatch between antenna and mixer, a part of the reverse radiation noise power is directly reflected back into the mixer, while the rest is radiated to the outside through antenna and afterwards reflected by objects of being imaged and finally received by antenna again. On account of the fact that the narrowband LO source leakage forms the crucial part of reverse radiation noise, the reverse radiation noise can be recognized as monochrome signal, and there is correlative relationship between the noise power reflected from objects and that reflected straightforward into mixer. Therefore, the interference phenomenon that usually occurs in active imaging systems appears here, and it is defined as interference-like effects in this paper.

Let Γ_a and Γ_t be the voltage reflection coefficients of antenna aperture and object, respectively. Assuming that the voltage of the reverse radiation noise at the RF port of mixer is E_{RN} , the voltage of the noise reflected directly back into mixer can be written as:

$$E_1 = |\Gamma_a E_{RN}| \exp(j\phi_1) \quad (13)$$

In addition, the voltage of the noise reflected from objects is expressed by:

$$E_2 = |(1 - \Gamma_a^2)\Gamma_t E_{RN} \sqrt{\psi}| \exp(j\phi_2) \quad (14)$$

Thus the superposition of these two components can be described by the following expression:

$$E_P = E_1 + E_2 \quad (15)$$

After a noise power to radiometric temperature transform of the square of Equation (15), the additional equivalent noise temperature arising from reverse radiation noise is given by:

$$T'_{RR} = T_{RN} \left[\Gamma_a^2 + (1 - \Gamma_a^2)^2 \Gamma_t^2 \psi + 2\Gamma_a \Gamma_t (1 - \Gamma_a^2) \sqrt{\psi} \cos \Phi \right] \quad (16)$$

where $\Phi = \phi_1 - \phi_2$ denotes the phase difference, and $\rho_t = \Gamma_t^2$. When $\Gamma_t = 1$, the normalized receiving temperature of reverse radiation noise can be defined as:

$$T'_{RA} = T'_{RR}|_{\Gamma_t=1} = T_{RN} \left[\Gamma_a^2 + (1 - \Gamma_a^2)^2 \psi + 2\Gamma_a(1 - \Gamma_a^2) \sqrt{\psi} \cos \Phi \right] \quad (17)$$

Considering Equation (17), the third part in the square brackets, representing the coherent component of reverse radiation noise, is the primary cause of interference-like effects. In addition, the extent of this influence is relevant to the reverse radiation noise at RF port T_{RN} , the voltage reflection coefficient at the antenna aperture Γ_a , and the receiving factor ψ . If we want to eliminate or reduce the effects of reverse radiation noise on imaging performance, the three parameters discussed above should be investigated. From Equations (2) and (3), it is evident that T_{RN} is proportional to ζ_{IF} and inversely proportional to L_{OR} . Meanwhile, Γ_a is directly proportional to the antenna's VSWR, the improvement of which is advantageous to imaging performance. From the definition of ψ , it is obvious that increasing the detection distance R can reduce the effects of reverse radiation noise to a certain extent, whereas the spatial resolution of imaging system will decrease if the half-power beamwidth $\theta_{3\text{dB}}$ is fixed.

Besides improving the performance of LO, antenna, and mixer, an isolator can be utilized between the antenna and the receiving channel. The isolator acts as a low-loss attenuator in the forward transmission direction, while it becomes a high-loss attenuator in the reverse transmission direction and can prevent the flow of noise power from transmitting into antenna. On the basis of Equations (2) and (3), when $P_{LO} = 10$ dBm, $L_{OR} = 30$ dB, $\zeta_{IF} = -160$ dBc/Hz, and $T_0 = 300$ K, the reverse radiation noise arriving at the RF port of mixer can be calculated and the result is $T_{RN} = 744$ K. Moreover, when an isolator with an isolation degree of 18 dB is employed in the system, the result will be $T_{RN} = 602$ K. Figure 2 shows the simulated normalized receiving temperature of reverse radiation noise T'_{RA} varying with the phase difference Φ when $T_{RN} = 744$ K and $T_{RN} = 602$ K, under the conditions of $G = 30$ dB, $\lambda = 3$ mm, $R = 1$ m, $\Gamma_a = 0.11$ and $\theta_{3\text{dB}} = 1.5^\circ$. From Figure 2, it can be seen that T'_{RA} changes with Φ regularly. This effect can give rise to interference-like stripes, which are disadvantageous to the detection and recognition of objects. In addition, adopting an isolator can reduce the reverse radiation noise.

Additionally, adopting an isolator has the advantages of simple operation and low cost. The approach of installing a low noise amplifier (LNA) in the MMW front-end is also feasible, but the high cost and the complex configuration have combined to make it difficult to realize the goal of high reliability and reasonable performance price

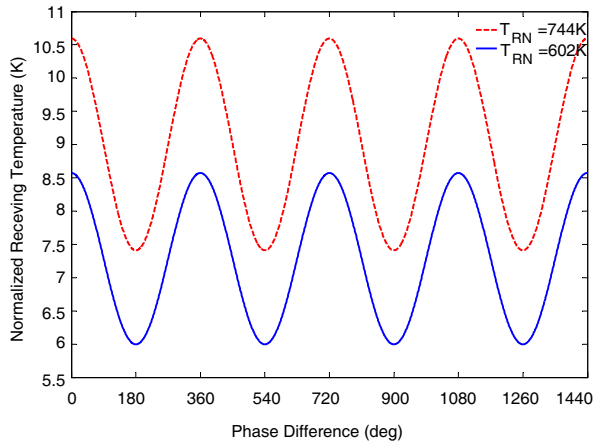


Figure 2. Normalized receiving temperature of reverse radiation noise versus phase difference.

ratio. Consequently, the method of adopting an isolator in the MMW receiving front-end is selected in this paper.

4. IMAGING EXPERIMENTS

For validating the specific influence of reverse radiation noise on imaging performance, and verifying the feasibility and significance of the method proposed above, two series of comparative imaging experiments are carried out by means of the radiometric imaging system designed and implemented in our laboratory. The parameters of the system are given as follows: center frequency $f = 94.5$ GHz, IF bandwidth $B = 3$ GHz, integration time $\tau = 50$ ms, and radiometric sensitivity $\Delta T = 0.4$ K. When the detection distance $R = 1$ m and the half-power beamwidth $\theta_{3\text{dB}} = 1.5^\circ$, the spatial resolution $\beta = 2.6$ cm.

The imaging experiments are conducted indoors, with the objects of interest placed on the experimental platform that is made of bare metal plate. The platform is mounted on a tripod and positioned near the windows of laboratory. With an adjustable angle between the normal of the platform and the vertical plane, the radiometric temperature of sky can be reflected into the imaging scene. Meanwhile, the objects with bare surfaces that are perpendicular to the horizontal plane mainly reflect the radiometric temperature of surroundings. According to [8], the radiometric temperature of surroundings is much higher than that of sky, thus the profiles of objects will stand out from the background.

The object in the first imaging experiment is a simulative gun tailored from a piece of metal plate, whose visible light image is shown in Figure 3(a). With our MMW radiometric imaging system, the radiometric image of the simulative gun is illustrated in Figure 3(b), and it is apparent that some interference-like stripes appear at the region of the object. These stripes, which are generated by the reverse radiation noise when there is no isolator in the MMW receiving front-end, result in a dim outline of the simulative gun and make it difficult for recognizing. In addition, an isolator with the isolation degree of 18 dB is put between the antenna and the mixer, and the corresponding MMW radiometric image is presented in Figure 3(c). Based upon the visual observation, it can be observed that the profile in Figure 3(c) is distinct and the imaging performance is improved considerably. Moreover, it is worth noting that due to the bare surface of experimental platform, the mirror images also emerge in both Figures 3(b) and 3(c), and then the quasi-optical characteristics of MMW are verified indirectly.

As displayed in Figure 4(a), the object in the second imaging experiment is a long metal plate with four large square holes and many other small holes. The reason for selecting such an object is to test the spatial resolution of the imaging system simultaneously. The long metal plate mainly reflect the radiometric temperature of surroundings, whereas the radiometric temperature of sky transmits through the holes, and the corresponding regions in MMW radiometric images will be blacker than that of the metal plate. Figure 4(b) demonstrates the MMW radiometric image when there is no isolator in the imaging system, and it is evident that there exist interference-like stripes, which lead to the failure of recognizing the second and the third large square holes. The MMW radiometric image presented in Figure 4(c) is acquired under the condition of installing an isolator in the imaging system. Comparing Figure 4(c) with Figure 4(b), the stripes are effectively eliminated, and the profile of the long metal plate

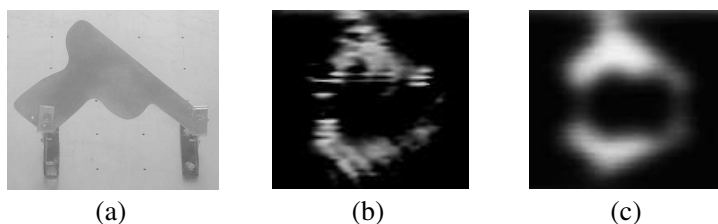


Figure 3. Imaging experiment of a simulative gun. (a) Visible light image. (b) Without isolator. (c) With isolator.

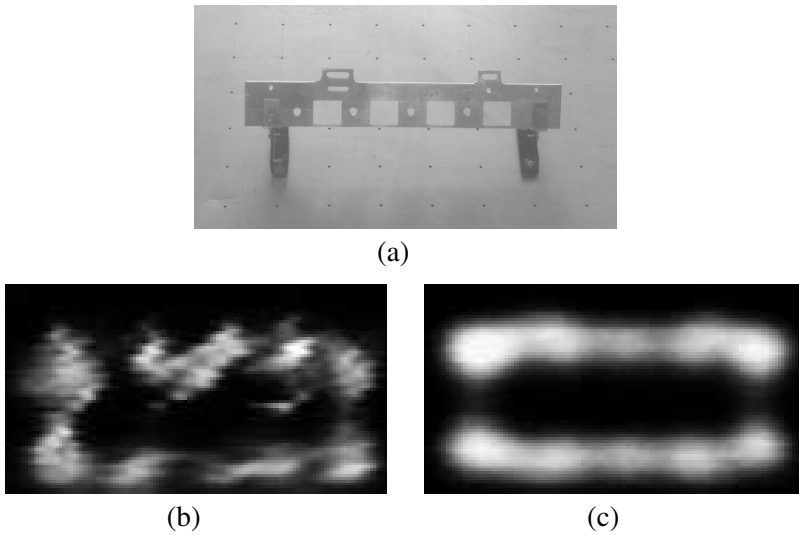


Figure 4. Imaging experiment of a long metal plate. (a) Visible light image. (b) Without isolator. (c) With isolator.

is more prominent. As a result of the fact that the dimensions of the bottom edges of the four large square holes are much smaller than the spatial resolution of the imaging system, the bottom edges are not interpretable in the radiometric image. Nevertheless, it is easy for us to distinguish the positions of the four holes, and even the two noses in the upper part of the metal plate are interpretable.

In summary, employing an isolator in the MMW receiving front-end can considerably reduce the effects of reverse radiation noise, and it is advantageous to the acquisition of high-quality MMW radiometric images. Moreover, other ways of exploiting low-noise high-stability LO, improving the VSWR of antenna, and enhancing the isolation between each port in mixer are all of benefit to the imaging performance.

5. CONCLUSION

The reverse radiation noise is a common phenomenon in the total-power superheterodyne MMW radiometric imaging system, and the effects of reverse radiation noise on MMW radiometric imaging for relative radiometry at short range have been investigated in this paper. Both the theoretical analysis and experimental results indicate that: (1) It is difficult to measure the reverse radiation noise accurately, and the value of this noise is not only related with the mismatch

of components in the receiving front-end, but also relevant to the property of LO, especially the modulation and narrowband noise arising from power leakage. (2) The method of adopting an isolator in the receiving front-end improves the image quality. And then, the high-quality images are beneficial to the feature extraction and target recognition in further studies. (3) The interference-like stripes caused by the coherent component indicate that the illumination source, which is utilized in the application of enhancing the radiometric temperature contrast between objects and backgrounds via artificial methods, should have the properties of broadband, homogeneous and non-directional. Additionally, exploring the relationship between the strip spacing and the operating wavelength, and improving both the stability and spatial resolution of the imaging system, are just the direction of further research.

ACKNOWLEDGMENT

This work is partially supported by the Specialized Research Fund for the Doctoral Program of Higher Education (No. 20093219120018), the China Postdoctoral Science Foundation Funded Project (No. 201004-81151), the Jiangsu Planned Projects for Postdoctoral Research Funds (No. 0801012C), the Development Fund of Nanjing University of Science and Technology (No. XKF09071), and the NUST Research Funding (No. 2011YBXM73). The authors also gratefully acknowledge the helpful comments and suggestions of the reviewers, which have improved the presentation.

REFERENCES

1. Yujiri, L., M. Shoucri, and P. Moffa, "Passive millimeter-wave imaging," *IEEE Microwave Magazine*, Vol. 4, No. 3, 39–50, 2003.
2. Boettcher, E. J., K. Krapels, R. Driggers, J. Garcia, C. Schuetz, J. Samluk, L. Stein, W. Kiser, A. Visnansky, J. Grata, D. Wikner, and R. Harris, "Modeling passive millimeter wave imaging sensor performance for discriminating small watercraft," *Applied Optics*, Vol. 49, No. 19, E58–E66, 2010.
3. Appleby, R. and R. N. Anderton, "Millimeter-wave and submillimeter-wave imaging for security and surveillance," *Proceedings of IEEE*, Vol. 95, No. 8, 1683–1690, 2007.
4. Oka, S., H. Togo, N. Kukusu, and T. Nagatsuma, "Latest trends in millimeter-wave imaging technology," *Progress In Electromagnetics Research Letters*, Vol. 1, 197–204, 2008.

5. Yeom, S., D.-S. Lee, H. Lee, J.-Y. Son, and V. P. Guschin, "Distance estimation of concealed objects with stereoscopic passive millimeter-wave imaging," *Progress In Electromagnetics Research*, Vol. 115, 399–407, 2011.
6. Hung, C. Y., M. H. Weng, R. Y. Yang, and H. W. Wu, "Design of a compact CMOS bandpass filter for passive millimeter-wave imaging system application," *Journal of Electromagnetic Waves and Applications*, Vol. 23, No. 17–18, 2323–2330, 2009.
7. Thakur, J. P., W.-G. Kim, and Y.-H. Kim, "Large aperture low aberration aspheric dielectric lens antenna for W-band quasi-optics," *Progress In Electromagnetics Research*, Vol. 103, 57–65, 2010.
8. Ulaby, F. T., R. K. Moore, and A. K. Fung, *Microwave Remote Sensing: Active and Passive, Volume I: Fundamentals and Radiometry*, Addison-Wesley Publishing Company, Massachusetts, 1981.
9. Peng, S.-S., Z.-C. Xu, and X.-G. Li, "Effect of inverse radiation noise of microwave radiometer for remote sensing on antenna temperature calibration," *Journal of Microwaves*, Vol. 13, No. 2, 108–113, 1997.
10. Li, J. and J.-S. Jiang, "Reverse radiation in microwave radiometer," *Journal of Remote Sensing*, Vol. 2, No. 4, 241–244, 1998.
11. Li, Z.-P., D.-M. Zhao, and J.-G. Miao, "Simulation study of the effect on inverse radiation thermal noise of microwave radiometer on antenna calibration," *Remote Sensing Technology and Application*, Vol. 22, No. 2, 268–271, 2007.
12. Xiao, Z.-L., T.-Y. Hu, J.-Z. Xu, and L. Wu, "Millimetre-wave radiometric imaging for concealed contraband detection on personnel," *IET Image Processing*, Vol. 5, No. 5, 375–381, 2011.